Crystalline Order on a Sphere and the Generalized Thomson Problem

M. Bowick,[1] A. Cacciuto,[1] D. R. Nelson,[2] and A. Travesset[3]
[1]*Physics Department, Syracuse University, Syracuse, New York 13244-1130*
[2]*Lyman Laboratory of Physics, Harvard University, Cambridge, Massachusetts 02138*
[3]*Loomis Laboratory, University of Illinois at Urbana, Urbana, Ilinois 61801*
(Received 11 June 2002; published 10 October 2002)

We attack the *generalized* Thomson problem, i.e., determining the ground state energy and configuration of many particles interacting via an arbitrary repulsive pairwise potential on a sphere via a continuum mapping onto a universal long range interaction between angular disclination defects parametrized by the elastic (Young) modulus Y of the underlying lattice and the core energy E_{core} of an isolated disclination. Predictions from the continuum theory for the ground state energy agree with numerical simulations of long range power law interactions of the form $1/r^{\gamma}$ $(0 < \gamma < 2)$ to four significant figures. The generality of our approach is illustrated by a study of grain boundary proliferation for tilted crystalline order and square lattices on the sphere.

DOI: 10.1103/PhysRevLett.89.185502 PACS numbers: 61.72.Mm, 61.72.Bb, 64.60.Cn, 82.70.Dd

The Thomson problem [1] of determining the ground state of classical electrons interacting with a repulsive Coulomb potential on the surface of a sphere is an almost 100-year-old puzzle [2] with many important physical realizations including multielectron bubbles [3] and surface ordering of liquid metal drops confined in Paul traps [4]. Although the original Thomson problem refers to the ground state of spherical shells of electrons, one can also ask for crystalline ground states of particles interacting with arbitrary potentials. Such a generalized Thomson problem arises, for example, in determining the arrangements of the protein subunits which comprise the shells of spherical viruses [5]. Here, the "particles" are clusters of protein subunits arranged on a shell. Other realizations include regular arrangements of colloid particles in *colloidosomes* [6] proposed for encapsulation of active ingredients such as drugs, nutrients, or living cells [7] and fullerene patterns of carbon atoms [8]. An example with long range logarithmic ($\gamma = 0$) interactions is provided by the Abrikosov lattice of vortices which would form at low temperatures in a superconducting metal shell with a large monopole at the center [9]. In practice, the "monopole" could be approximated by the tip of a long thin solenoid.

Extensive numerical studies of the Thomson problem show that the ground state for a small number of particles, typically $M \leq 150$, contains 12 five-coordinated particles (elementary charge $+1$ disclinations [10,11]) located at the vertices of an icosahedron [12]. All other particles have coordination number 6, as for planar triangular packing. At least 12 charge $+1$ disclinations are required by a classical theorem of Euler equating the total disclination charge to 6χ, where the Euler characteristic χ is 2 for the sphere [13]. Recent results have shown that, for systems as small as 500 particles, however, configurations with *excess* dislocations [14,15] have *lower* energies than icosahedral ones.

These remarkable results for the Thomson problem raise a number of important questions, such as the mechanism behind the proliferation of defects, the nature of these unusual low-energy states, the universality with respect to the underlying particle potential, and the generalization to more complex situations.

A formalism suitable to address all these questions has been proposed recently [16]. Disclinations are considered the fundamental degrees of freedom, interacting according to the energy,

$$H = E_0 + \frac{Y}{2}\iint d\sigma(x)d\sigma(y) \times \left\{[s(x) - K(x)]\frac{1}{\Delta^2}[s(y) - K(y)]\right\}, \qquad (1)$$

where the integration is over a fixed surface with area element $d\sigma(x)$ and metric g_{ij}, K is the Gaussian curvature, Y is the Young modulus in flat space, and $s(x) = \sum_{i=1}^{N} \frac{\pi}{3} q_i \delta(x, x_i)$ is the disclination density [$\delta(x, x_i) = \delta(x - x_i)/\sqrt{\det(g_{ij})}$]. Here five- and sevenfold defects correspond to $q_i = +1$ and -1, respectively. Defects such as dislocations or grain boundaries can be built from these N elementary disclinations. E_0 is the energy corresponding to a perfect defect-free crystal with no Gaussian curvature; E_0 would be the ground state energy for a 2D Wigner crystal of electrons in the plane. Equation (1) restricted to a sphere gives [16]

$$H = E_0 + \frac{\pi Y}{36} R^2 \sum_{i=1}^{N}\sum_{j=1}^{N} q_i q_j \chi(\theta^i, \psi^i; \theta^j, \psi^j) + N E_{\text{core}}, \qquad (2)$$

where E_{core} is a defect core energy, R is the radius of the sphere, and χ is a function of the geodesic distance β_{ij} between defects with polar coordinates $(\theta^i, \psi^i; \theta^j, \psi^j)$: $\chi(\beta) = 1 + \int_0^{(1-\cos\beta)/2} dz \frac{\ln z}{1-z}$. In this Letter, we show

that the continuum formalism embodied in Eq. (2) implies (i) flat space results for elastic constants can be bootstrapped into very accurate quantitative calculations for generalized Thomson problems, thus providing a stringent test of the validity of this approach; (ii) new results for finite length grain boundaries, consisting of dislocations with variable spacing, in the context of 2π disclinations studied in tilted liquid crystal phases [17]; and (iii) enough generality to determine the ground state for the eight minimal disclinations arising in *square* tilings of a sphere.

The Young modulus Y and the energy E_0 may be computed in flat space via the Ewald method [18]. The result for M particles with long range pairwise interactions given by e^2/r^γ $(0 < \gamma < 2)$ is

$$Y = 4\eta(\gamma)\frac{e^2}{A_C^{1+\gamma/2}},$$
$$\frac{E_0}{Me^2} = \theta(\gamma)\left(\frac{4\pi}{A_C}\right)^{\gamma/2} + \frac{\pi}{A_C R^{\gamma-2}}\rho(\gamma), \tag{3}$$

where η, θ, and ρ are potential-dependent coefficients, and A_C is the area per particle. For M particles crystallizing on the sphere, $A_C = 4\pi R^2/M$, and combining Eqs. (2) and (3) gives a large M expansion for the ground state energy,

$$E_G = \frac{e^2}{2R^\gamma}[a_0(\gamma)M^2 - a_1(\gamma)M^{1+(\gamma/2)} + a_2(\gamma)M^{\gamma/2} + \ldots], \tag{4}$$

where $a_0(\gamma) = 2^{1-\gamma}/(2-\gamma)$ and the subleading coefficients $a_i(\gamma)$ depend explicitly on the potential and on the positions and number of disclinations. The first (nonextensive) term is proportional to M^2 and is usually canceled by a uniform background charge for Wigner crystals of electrons. The coefficient a_1 is a universal function of the positions of the defects, up to a potential-dependent constant. Theoretical predictions [16] for large M for icosadeltahedral lattices of type $(n, 0)$ and (n, n) [5,19] are given in Table I for five values of γ.

These predictions may now be compared with direct minimizations of icosadeltahedral configurations on the sphere by fitting the results to Eq. (4). In Fig. 1, we plot $\varepsilon(M)$ versus $1/M$ for $(n, 0)$ and (n, n) icosadeltahedral configurations for $\gamma = 1.5$ and $\gamma = 0.5$, where

$$\varepsilon(M) = \frac{[2R^\gamma E_G/e^2 - a_0(\gamma)M^2]}{M^{1+\gamma/2}}. \tag{5}$$

The coefficient $a_1(\gamma)$ is determined by the intercept in the $M \to \infty$ limit [$M = 10n^2 + 2$ for $(n, 0)$ lattices and $M = 30n^2 + 2$ for (n, n) lattices [5]].

The continuum elastic interaction between disclinations in Eq. (2) is essential to obtain the correct limiting behavior since $a_1(\gamma)$ reflects contributions both from the energy per particle in flat space as well as the energies of 12 isolated disclinations. The core energy term in Eq. (2) contributes to the leading correction $a_2(\gamma)$. We find agreement to four significant figures for $(n, 0)$ icosadeltahedral lattices and to five significant figures for (n, n) lattices. The small residual difference in energy for $(n, 0)$ and (n, n) configurations may be understood from the differing strain energies shown in Fig. 2.

Another illustration of the power of our continuum approach is provided by showing that Eq. (2) implies the proliferation of grain boundary arrays for sufficiently large system size. We illustrate the method [16] by considering just two 2π defects (appropriate to crystals of tilted molecules [17]) with suitable boundary conditions. To approximate the 2π disclination of tilted molecules in a hemispherical crystal [17], we replace the icosahedral configuration of 12 disclinations with two clusters of six $2\pi/6$ defects at the north and south poles. For simplicity, we use isotropic elastic theory and neglect nonuniversal details near the core of the $+2\pi$ disclination. Upon adding just one dislocation of Burgers vector [10,20] b (i.e., a $\pm 2\pi/6$ disclination pair separated by distance b), the minimum energy in Eq. (2) is achieved by a polar angle $\theta_0(b)$ with $\vec{b}$ perpendicular to the geodesic joining the north and south poles. For small numbers of dislocations, the minimum energy configuration consists of two polar

TABLE I. Analytical predictions (first column) for a large number of particles and values extrapolated from numerical simulations (second and third columns) of the coefficient $a_1(\gamma)$, as defined in Eq. (4) for (n, n) and $(n, 0)$ icosadeltahedral lattices. Similar accuracy holds for other values of γ.

γ	$a_1(\gamma)$	(n, n)	$(n, 0)$
1.5	1.514 73	1.514 54(2)	1.514 45(2)
1.25	1.226 17	1.225 99(7)	1.225 89(7)
1.0	1.104 94	1.104 82(3)	1.104 64(3)
0.75	1.049 40	1.049 21(6)	1.049 10(6)
0.5	1.023 92	1.023 90(4)	1.023 72(4)

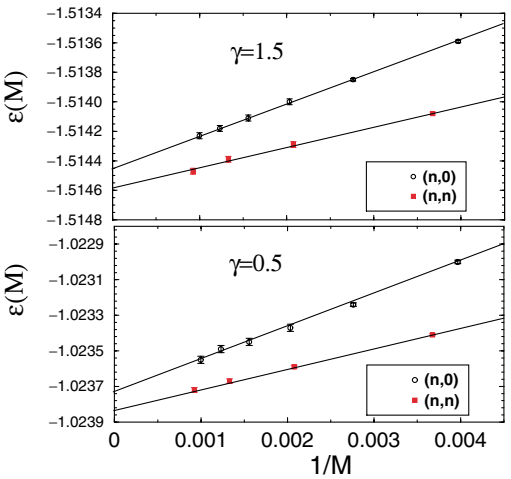

FIG. 1 (color online). Numerical estimate of $\varepsilon(M)$ as a function of $1/M$ for $(n, 0)$ and (n, n) icosadeltahedral lattices with $\gamma = (1.5, 0.5)$.

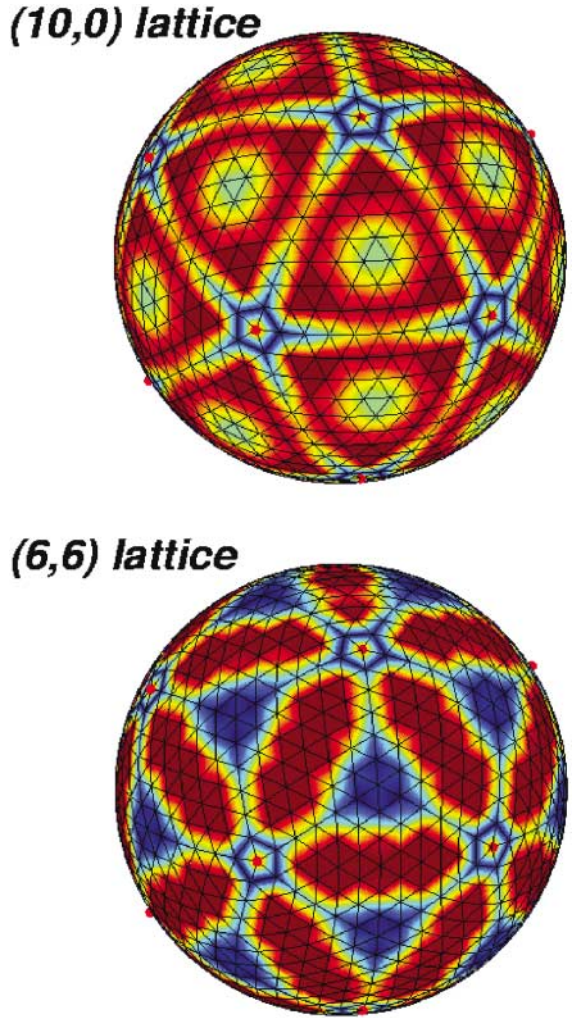

FIG. 2 (color). Strain energy distribution (red/high, blue/low) for a (10,0) and a (6,6) configuration.

rings of dislocations located at angles $\theta_0(b)$ and $\pi - \theta_0(b)$ relative to the north pole. The dislocations eventually organize into grain boundaries centered on $\theta_0(b)$, as shown in Fig. 3. Remarkably, no other minima were found.

Because the global minimization just described becomes computationally demanding for more than 30 defects, further minimizations focused on a reduced parameter space specified by the orientations and distances of the grain boundaries from the two +6 defects. Following [16], the system *dynamically* chooses the average lattice spacing $a \equiv b$ that best accommodates the array structure by extremizing the energy of Eq. (2).

For reasonable parameter values in our continuum description, both two antipodal +6 disclinations and the icosadeltahedral configurations are indeed unstable to the formation of grain boundaries for sufficiently large sphere radius [14–16,21]. In a flat monolayer, the spacing l between dislocations in m-grain boundary arms radiating from a disclination of charge s is given by $l/b = 2\sin(\frac{s}{2m})$[20], where b is the Burgers vector charge. The

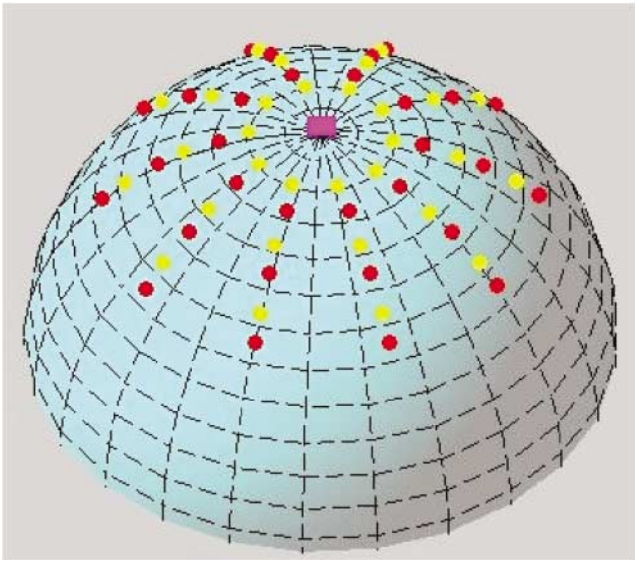

FIG. 3 (color). A ten-arm grain boundary array emerging from a +6 defect (purple square) at the north pole. Charge +1 disclinations are red and charge −1 disclinations are yellow.

disclination charge is $s = \frac{2\pi}{6} p$ ($p = 1$ or 6, corresponding to the Thomson problem or tilted molecules, respectively). To generalize this result for symmetrical grain boundaries on a sphere, consider the Burgers circuit formed by an isosceles spherical triangle with apex angle $\phi_{gb} = s/m$ at a disclination at the north pole and centered on one of the m-grain boundary arms [22]. If the altitude of this triangle is h, the net Burgers vector B defined by this circuit is given by the geodesic distance spanning the base of this triangle. A straightforward exercise in spherical trigonometry leads to

$$\cos\left(\frac{B}{R}\right) = \frac{\cot^2(h/R)\cos^2(\phi_{gb}/2) + \cos(\phi_{gb})}{1 + \cot^2(h/R)\cos^2(\phi_{gb}/2)}. \quad (6)$$

Writing $B \approx b\int_0^h dh'/l(h')$, where $l(h)$ is a (variable) dislocation spacing [16], we can invert this formula and thus generalize the dislocation spacing result above.

Results comparing our minimization with Eq. (6) are shown in Fig. 4. Both approaches predict the same number of dislocations within a grain and dislocation spacings which *increase* with θ [16]. The small discrepancies in the positions of the dislocations are presumably due to interactions between dislocations in different arms.

The physics associated with Eq. (2) is remarkably general. We sketch here how the results above may be adapted to a sphere tiled with a *square* lattice. A planar square lattice is described by three elastic constants (as opposed to the two Lamé coefficients in the triangular case), leading to an energy

$$H = \frac{\lambda_{\alpha\beta,\mu\nu}}{2}\int d^2\mathbf{x} u_{\alpha\beta} u_{\mu\nu}, \quad (7)$$

where the independent elastic constants are $\lambda_{11,11}$, $\lambda_{11,22}$,

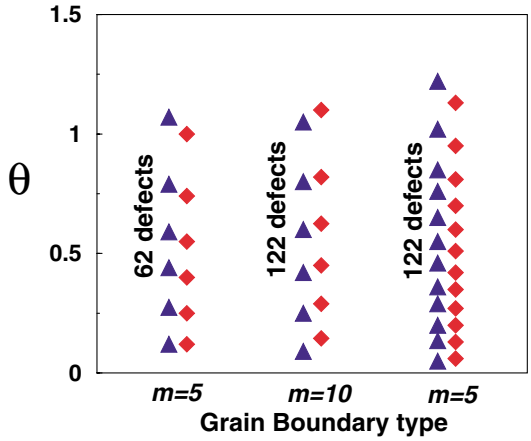

FIG. 4 (color online). Defect positions obtained from minimization (up triangle) and from Eq. (6) (diamonds).

and $\lambda_{12,12}$. The same derivation as that leading to Eq. (1) now leads to

$$H = \frac{1}{2}\int d\sigma(x) d\sigma(y)[K(x) - s(x)]G(x, y)[K(y) - s(y)], \tag{8}$$

where $G(x, y) = (\frac{1}{Y}\Delta^2 + 2\epsilon\nabla_1^2\nabla_2^2)^{-1}$, with ∇_i the gradient in direction $i = 1$ or 2, as defined by the local square lattice. The fundamental defects are now $\pm\frac{\pi}{2}$ disclinations. The elastic constants are

$$Y = \frac{\lambda_{11,11}^2 - \lambda_{11,22}^2}{\lambda_{11,11}}, \qquad \epsilon = -\frac{\lambda_{11,22} + \lambda_{11,11}}{\lambda_{11,11}^2 - \lambda_{11,22}^2} + \frac{1}{2\lambda_{12,12}}. \tag{9}$$

The interaction energy for disclinations in a square lattice becomes equivalent to Eq. (1) only in the limit $\epsilon = 0$. Although details such as the critical value of R/a for the onset of grain boundaries will differ, we expect that the physics remains essentially the same. For small numbers of particles, the ground state will consist of eight $q = +1$ disclinations. In the isotropic case ($\epsilon = 0$), the ground state is a distorted cube, with one face twisted by 45°, similar to tetratic liquid crystal ground states on the sphere [23].

We expect similar results for geometries other than the sphere. For isotropic crystals on a torus with the right aspect ratio, for example, one might expect 12 fivefold disclinations on the outer wall (where the Gaussian curvature is positive) and 12 compensating sevenfold disclinations on the inner wall (where the Gaussian curvature is negative) to play the role of the icosahedral configurations on the sphere. As more particles are placed on the torus, we expect grain boundaries to emerge from these disclinations.

We thank Alar Toomre for sharing with us his numerical work on the original Thomson problem. The work of M. B. and A. C. has been supported by the U.S. DOE under Contract No. DE FG02 85ER40237. The research of D. R. N was supported by the NSF through Grant No. DMR97-14725 and through the Harvard Material Research Science and Engineering Laboratory via Grant No. DMR98-09363. The work of A. T. has been supported by the Materials Computation Center and Grants No. NSF-DMR 99-76550 and No. NSF-DMR 00-72783.

[1] J. J. Thomson, Philos. Mag. **7**, 237 (1904).
[2] E. B. Saff and A. B. J. Kuijlaars, Math. Intelligencer **19**, 5 (1997).
[3] P. Leiderer, Z. Phys. B **98**, 303 (1993).
[4] E. J. Davis, Aerosol Sci. Technol. **26**, 212 (1997).
[5] D. L. D. Caspar and A. Klug, Cold Spring Harbor Symp. Quant. Biol. **27**, 1 (1962).
[6] M. Nikolaides, thesis, TU Munich, 2001.
[7] A. D. Dinsmore *et al.* (to be published).
[8] H. W. Kroto *et al.*, Nature (London) **318**, 162 (1985).
[9] M. J. W. Dodgson and M. A. Moore, Phys. Rev. B **55**, 3816 (1997).
[10] R. Cotterill, *The Cambridge Guide to the Material World* (Cambridge University Press, Cambridge, England, 1985).
[11] P. M. Chaikin and T. C. Lubensky, *Principles of Condensed Matter Physics* (Cambridge University Press, Cambridge, England, 1995).
[12] T. Erber and G. M. Hockney, Adv. Chem. Phys. **98**, 495 (1997).
[13] H. G. Flegg, *From Geometry to Topology* (Dover, New York, 2001).
[14] A. Toomre (private communication).
[15] A. Perez-Garrido and M. A. Moore, Phys. Rev. B **60**, 15 628 (1999), and references therein.
[16] M. Bowick, D. R. Nelson, and A. Travesset, Phys. Rev. B **62**, 8738 (2000).
[17] R. Pindak, S. B. Dierker, and R. B. Meyer, Phys. Rev. Lett. **56**, 1819 (1986); by introducing a pressure difference across the free standing liquid crystal film, one could study the 2π disclinations and grain boundaries of this reference in a hemispherical environment [R. Pindak and C. C. Huang (private communication)].
[18] L. Bonsall and A. A. Maradudin, Phys. Rev. B **15**, 1959 (1977).
[19] For a type (n, m) icosadeltahedral lattice, one reaches a neighboring disclination from a given one by taking n steps along the lattice in one direction, turning 120°, and continuing m steps.
[20] J. P. Hirth and J. Lothe, *Theory of Dislocations* (Wiley, New York, 1982).
[21] For the purposes of determining grain boundary stability, it is useful to write the core energy term $E_{\rm core}$ in Eq. (2) as $NE_{\rm core} = 12E_5 + \frac{N-12}{2}E_d$ and parametrize the physics in terms of a dislocation core energy E_d of order $0.1Ya^2$. For antipodal +6 defects, $NE_{\rm core} = 2E_{+6} + \frac{N-2}{2}E_d$.
[22] C. Carraro and D. R. Nelson, Phys. Rev. E **48**, 3082 (1993).
[23] T. C. Lubensky and J. Prost, J. Phys. II (France) **2**, 371 (1992).